

# ESTIMATING EMISSIONS OF 20 VOCs.

## II: DIFFUSED AERATION

By Chu-Chin Hsieh,<sup>1</sup> Roger W. Babcock Jr.,<sup>2</sup> Student Member, ASCE, and Michael K. Stenstrom,<sup>3</sup> Member, ASCE

**ABSTRACT:** A relationship developed in a companion paper to estimate emissions from surface-aerated reactors that accounts for both gas- and liquid-phase mass-transfer resistances is extended to reactors with diffused-aeration systems. The method accurately predicts the observed stripping rate of 20 volatile organic compounds (VOCs) with a wide range of Henry's coefficients over a wide range of hydrodynamic conditions. The degree of gas saturation and the liquid- and gas-phase mass-transfer coefficients are estimated.

### INTRODUCTION

The popular approach of using the oxygen-transfer coefficient and the ratio of molecular diffusivities (defined as  $\Psi$ ) to predict emission rates of volatile organic compounds (VOCs) in natural water and aeration systems is restricted to highly volatile compounds, such as trichloroethylene and carbon tetrachloride. A modified  $\Psi$ , referred to as  $\Psi_M$ , extends this approach to a wide range of volatilities or Henry's coefficients ( $H_c$ ). Part 1 of this paper (Hsieh et al. 1993) developed the approach and showed its application to surface-aeration systems. The objective of this paper is to apply the approach to diffused-aeration systems by estimating oxygen gas-phase and liquid-phase mass-transfer coefficients. (This is the second paper in a three-part series; the third paper will describe turbine aeration, dimensional analysis, and the effect of surfactants on mass transfer.)

### BACKGROUND

Mass transfer in a diffused aeration system is a dynamic process in which the local equilibrium concentrations (the driving force) change as bubbles rise through the liquid column. The relationship between VOCs in the gas and liquid phases in a rising bubble was described by Matter-Muller et al. (1981) and Roberts et al. (1982). Their development included the following assumptions: the overall mass-transfer coefficient  $K_L a$  is constant during an experiment; equilibrium holds at the interface and is described by Henry's law; gas-flow rate and temperature are constant; the rising bubbles are distributed uniformly across the column; pressure and volume changes within the air bubbles are negligible; the liquid phase is well mixed (homogeneous); the liquid-phase concentration is time-dependent but remains constant during the residence time of a single bubble; and the gas-phase concentration is dependent on bubble-residence time and vertical position.

Based on gas-transfer principles (Matter-Muller et al. 1981; Robert et al.

---

<sup>1</sup>Sr. Engr., Montgomery Watson, Inc., P.O. Box 7009, Pasadena, CA 91109-7009.

<sup>2</sup>Sr. Engr., John Carollo Engrs., 450 N. Widget Ln., Walnut Creek, CA 94598.

<sup>3</sup>Prof., Civ. Engrg. Dept., Univ. of California, Los Angeles, CA 90024.

Note. Discussion open until May 1, 1994. Separate discussions should be submitted for the individual papers in this symposium. To extend the closing date one month, a written request must be filed with the ASCE Manager of Journals. The manuscript for this paper was submitted for review and possible publication on May 15, 1992. This paper is part of the *Journal of Environmental Engineering*, Vol. 119, No. 6, November/December, 1993. ©ASCE, ISSN 0733-9372/93/0006-1099/\$1.00 + \$.15 per page. Paper No. 4197.

1984) applied to diffused aeration, the gas-phase (bubble) and liquid-phase concentrations of for a rising bubble are related by

$$C_G = C_L H_c \left\{ 1 - \exp \left[ -\frac{K_L a (V_L)}{Q_G H_c} \left( \frac{t}{tr} \right) \right] \right\} \dots \dots \dots (1)$$

where  $C_G$  = gas-phase concentration (mg/L);  $C_L$  = liquid-phase concentration (mg/L);  $H_c$  = Henry's coefficient, the equilibrium relationship of solute between gas-phase and liquid-phase concentration (dimensionless);  $K_L a$  = overall liquid-phase mass-transfer coefficient ( $h^{-1}$ );  $V_L$  = liquid volume (L);  $Q_G$  = gas flow rate (L/h);  $t$  = retention time of the bubble rising through the liquid (h); and  $tr$  = total retention time of the bubble from diffuser to free water surface (h).

The VOC concentration in the air bubble as it exits at the free water surface ( $t = tr$ ) is

$$C_G = C_L H_c \left\{ 1 - \exp \left[ -\frac{K_L a (V_L)}{Q_G H_c} \right] \right\} \dots \dots \dots (2)$$

Roberts et al. (1984) defined the term in the square brackets of (2) as a saturation parameter ( $\phi Z_s$ ), where  $Z_s$  = submergence of the diffuser relative to the water surface as follows:

$$\phi Z_s = \frac{K_L a (V_L)}{Q_G H_c} \dots \dots \dots (3)$$

This parameter is a constant for each compound during any particular experiment because all the terms on the right-hand side are constant. For very large values of  $K_L a$  and small values of  $H_c$ , the bubble exit concentration approaches saturation.

Fig. 1 shows the relationship between bubble retention time ( $t$ ) and diffuser submergence ( $Z$ ), which is written as follows:

$$\frac{t}{tr} = \frac{Z_s - Z}{Z_s} \dots \dots \dots (4)$$

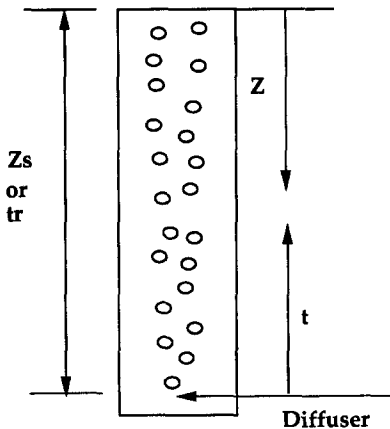


FIG. 1. Relationship between Diffuser Submergence and Bubble Retention Time

where  $Z$  = submergence of the bubble relative to the water surface (m).

Substituting (4) into (1), we obtain

$$C_G = C_L H_c \left\{ 1 - \exp \left[ -\phi(Z_s) \left( \frac{Z_s - Z}{Z_s} \right) \right] \right\} \dots \dots \dots (5)$$

which describes the change in gas-phase concentration of the VOCs as a function of submergence  $Z$ .

Eq. (2) can be used to describe the degree of saturation ( $S_d$ ) of a VOC in the bubble as follows:

$$S_d = \frac{C_G}{C_L H_c} = \frac{C_G}{C_G^*} = \left\{ 1 - \exp \left[ -\frac{K_L a(V_L)}{Q_G H_c} \right] \right\} \dots \dots \dots (6)$$

where  $C_G^* = C_L H_c$  = VOC concentration in the gas phase that would be in equilibrium with the liquid-phase VOC concentration (mg/L).

Fig. 2, calculated from (6), shows the degree of saturation ( $C_G/C_G^*$ ) (curved lines) of a VOC in a batch reactor as a function of the fraction of retention time ( $t/tr$ ) and the saturation parameter  $[K_L a(V_L)]/(Q_G H_c)$ . For a given diffused-aeration system and VOC, the saturation parameter ( $\phi Z_s$ ) is constant (Munz and Roberts 1984), thus the progress of bubble saturation as it rises to the surface is represented by following ( $t/tr$ ) from 0 to 1. For example, chloroform has a  $\phi Z_s$ -value of approximately 2.0 for the column shown in Fig. 1. As a bubble rises from the diffuser to the surface, the chloroform saturation increases from zero at ( $t/tr$ ) = 0 to 50% saturation at ( $t/tr$ ) = 0.35 to 70% saturation at ( $t/tr$ ) = 0.60 to about 85% saturation when the bubble reaches the surface.

We can use a liquid-phase mass balance to describe the transfer of VOCs from the liquid phase into the gas phase and derive an equation for the change of liquid-phase concentration from  $C_{L_o}$  to  $C_L$  during a period of time ( $t - t_o$ ), as follows:

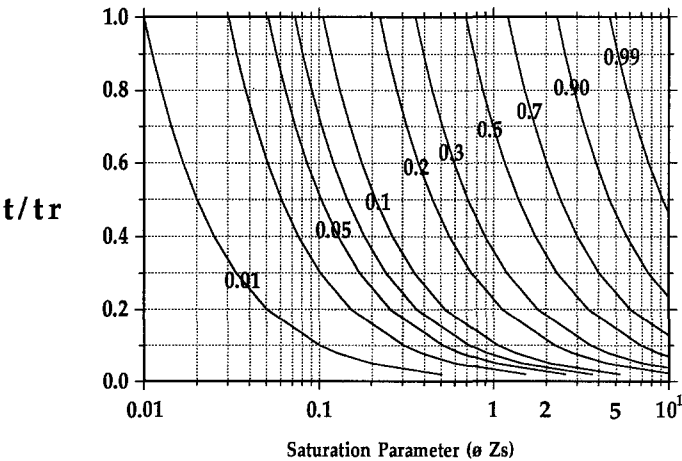


**FIG. 2. Degree of Saturation of Rising Bubbles ( $C_G/C_G^*$ , Curved Lines) as Function of Two Dimensionless Parameters**

$$\ln \left( \frac{C_L}{C_{Lo}} \right) = -\frac{Q_G H_c}{V_L} Sd(t - t_o) \dots \dots \dots (7)$$

A log-linear regression of the negative log of the concentration ratio  $[-\ln(C_L/C_{Lo})]$  versus time gives the following slope ( $Sp$ ):

$$Sp = \frac{Q_G H_c}{V_L} Sd \dots \dots \dots (8)$$

The mass-transfer rate coefficient for VOCs can be estimated from experimental results by substituting (6) into (8) and rearranging as follows:

$$K_{La} = -\frac{Q_G H_c}{V_L} \ln \left[ 1 - (Sp) \frac{V_L}{H_c Q_G} \right] \dots \dots \dots (9)$$

Substituting (8) into (9), we obtain

$$K_{La} = -Sp \left[ \frac{-\ln(1 - Sd)}{Sd} \right] \dots \dots \dots (10)$$

We can define the term in the square brackets of (10) as a transfer parameter ( $f_{KLa}$ ), which can be used to convert the slope of a log-linear regression of concentration ratio versus time into an emission rate. Thus, (10) can be simplified as follows:

$$K_{La} = -Sp f_{KLa} \dots \dots \dots (11)$$

where  $f_{KLa}$  = transfer parameter =  $[-\ln(1 - Sd)]/Sd$ . Matter-Muller et al. (1981) and Roberts et al. (1982) related the mass-transfer rate to three ranges of the saturation parameter. Using a similar approach, (11) can be simplified over three degree-of-saturation ranges using Fig. 3, which shows

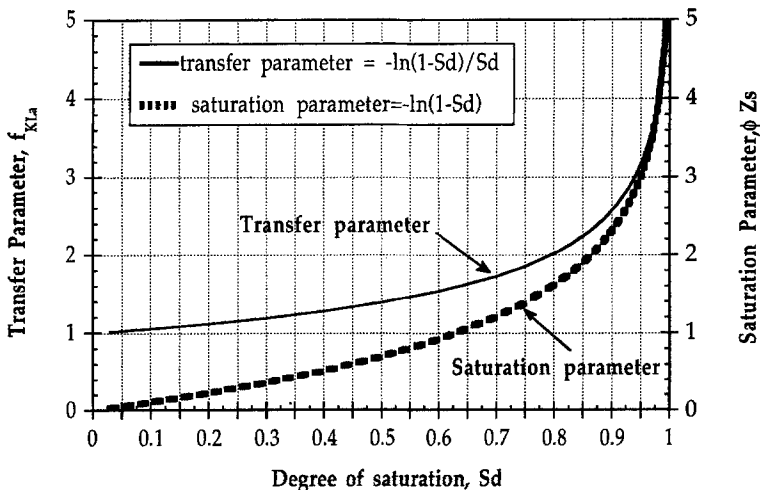


FIG. 3. Transfer and Saturation Parameters as Function of Degree of Saturation

$f_{K_{La}}$  and  $\phi Z_s$  as functions of the degree of saturation. Three cases are described.

**Case 1: For  $S_d \leq 0.1$**

The transfer parameter  $f_{K_{La}}$  is equal to 1.05 for  $S_d = 0.1$  and approaches 1 as  $S_d$  approaches zero. Therefore, the  $S_p$  is approximately equal to  $K_{La}$ , and (7) can be simplified to the following:

$$\ln \left( \frac{C_L}{C_{Lo}} \right) = -K_{La}(t - t_o) \dots\dots\dots (12)$$

This case is indicative of the situation in which the exit air is far from saturation (less than 10%). This may be the case for compounds with high  $H_c$ 's, such as oxygen, or for high air-flow rates ( $Q_G$ ). This situation is similar to VOC stripping in surface-aeration systems, in which the continuous and rapid renewal of fresh air above the water surface is provided, and saturation is negligible. Under these circumstances  $K_{La}$  may be calculated from (12) directly.

**Case 2: For  $S_d \geq 0.99$**

Since  $S_d \approx 1.0$ , (7) can be simplified as follows:

$$\ln \left( \frac{C_L}{C_{Lo}} \right) = -\frac{Q_G H_c}{V_L} (t - t_o) \dots\dots\dots (13)$$

This is the case in which the exit gas is saturated (>99%) with respect to the VOC being stripped. This may occur because of low values of  $H_c$  or long bubble-retention times. According to Matter-Muller et al. (1981), compounds that have high  $H_c$ 's, such as oxygen ( $H_c = 30.02$ ), may require at least 30 m of tank depth to attain saturation (or equilibrium). Conversely, compounds with small  $H_c$ 's, such as toluene ( $H_c = 0.24$ ), achieve saturation after rising only 0.8 m. Under these conditions (13) may be used for determining  $H_c$  as proposed by Mackay et al. (1979); however,  $K_{La}$  cannot be determined accurately, because a small change in exit-bubble saturation produces a large change in the transfer parameter and  $K_{La}$ .

**Case 3:  $0.1 < S_d < 0.99$**

Most applications fall within this case. The exit gas is partially saturated with the VOC (between 10% and 99% of saturation). Eqs. (7) and (11) must be used to describe this situation. The mass-transfer rate for the VOC is a function of the mass-transfer coefficient as well as the degree of saturation of the VOC in the exit air.

**$\Psi_M$  Concept**

Development of the  $\Psi_M$  concept was described previously (Hsieh et al. 1993). The concept is briefly summarized in the following. The mass-transfer coefficient of a VOC can be estimated from the product of  $\Psi_M$  and the  $K_{La}$  of oxygen as follows:

$$K_{La_{VOC}} = \Psi_M(K_{La_{O_2}}) \dots\dots\dots (14)$$

where  $\Psi_M$  = ratio of the mass-transfer coefficient of the VOC to oxygen

TABLE 1. Properties of 20 VOCs Studied (at 760 mmHg, 20°C)

Compound (1)	Formula (2)	Abbreviation (3)	Molecular weight (g) (4)	Solubility (S) (mg/L) (5)	Partial pressure (mmHg) (6)	Boiling point (°C) (7)	$H_c$ (8)
Benzene	C <sub>6</sub> H <sub>6</sub>	BZ	78.1	1,780.0	76.0	80.0	0.230
Bromobenzene	C <sub>6</sub> H <sub>5</sub> Br	BBZ	157.0	500.0	3.3	156.0	0.100
Bromoform	CHBr <sub>3</sub>	BF	252.8	3,033.0	5.6	149.5	0.041
Carbon tetrachloride	CCl <sub>4</sub>	CT	153.8	800.0	90.0	76.5	1.316
Chlorobenzene	C <sub>6</sub> H <sub>5</sub> -Cl	CBZ	112.6	500.0	8.8	132.0	0.150
Chloroform	CHCl <sub>3</sub>	CLF	119.4	8,000.0	160.0	61.7	0.160
1,2-Dichlorobenzene	C <sub>6</sub> H <sub>4</sub> Cl <sub>2</sub>	12DCB	147.0	100.0	1.0	179.0	0.087
1,3-Dichlorobenzene	C <sub>6</sub> H <sub>4</sub> Cl <sub>2</sub>	13DCB	147.0	111.0	1.49	173.0	0.120
1,4-Dichlorobenzene	C <sub>6</sub> H <sub>4</sub> Cl <sub>2</sub>	14DCB	147.0	79.0	0.6	174.0	0.110
1,2-Dichloroethene (cis)	CHCl=CHCl	12DCE	96.9	3,500.0	206.0	60.3	0.170
Ethylbenzene	C <sub>6</sub> H <sub>5</sub> -CH <sub>2</sub> CH <sub>3</sub>	EBZ	106.2	152.0	7.0	136.0	0.260
Ethylenebromide	CH <sub>2</sub> BrCH <sub>2</sub> Br	EDB	187.9	4,310.0	11.0	131.6	0.041
Naphthalene	C <sub>10</sub> H <sub>8</sub>	NAPH	128.2	30.0	0.011	217.9	0.038
Perchloroethylene	CCl <sub>2</sub> =CCl <sub>2</sub>	PCE	165.8	140.0	18.0	121.0	0.570
1,1,1-Trichloroethane	CCl <sub>3</sub> CH <sub>3</sub>	111TCA	133.4	720.0	100.0	74.1	0.530
1,1,2,2-Tetrachloroethane	CHCl <sub>2</sub> CHCl <sub>2</sub>	1122TCA	167.9	3,100.0	6.5	146.2	0.042
Toluene	C <sub>6</sub> H <sub>5</sub> -CH <sub>3</sub>	TLN	92.1	515.0	22.0	110.0	0.230
Trichloroethylene	CCl <sub>2</sub> =CHCl	TCE	131.4	1,100.0	58.0	87.0	0.250
1,2-Xylene (O)	C <sub>6</sub> H <sub>4</sub> -(CH <sub>3</sub> ) <sub>2</sub>	OXY	106.2	213.0	5.0	144.4	0.180
1,3-Xylene (m)	C <sub>6</sub> H <sub>4</sub> -(CH <sub>3</sub> ) <sub>2</sub>	MXY	106.2	146.0	6.0	139.0	0.240

(dimensionless); and  $K_L a_{\text{VOC}}$ ,  $K_L a_{\text{O}_2}$  = overall mass-transfer coefficients for the VOC and oxygen ( $\text{h}^{-1}$ ).

The value of  $\Psi_M$  can be estimated from the ratio of molecular diffusivities of the VOC and oxygen and the fraction of the liquid phase to overall mass-transfer resistance as follows:

$$\Psi_M = \Psi \frac{R_L}{R_T} = \left( \frac{D_{L\text{VOC}}}{D_{L\text{O}_2}} \right)^n \frac{R_L}{R_T} \dots\dots\dots (15)$$

where  $D_{L\text{VOC}}$ ,  $D_{L\text{O}_2}$  = liquid diffusivities for the VOC and oxygen ( $\text{m}^2/\text{s}$ ); and  $n$  = exponent, dependent on turbulence of liquid phase (dimensionless).

The fraction of liquid phase to overall mass-transfer resistance is determined by the  $H_c$  of the VOC and the gas-phase and liquid-phase mass-transfer coefficients as follows:

$$\frac{R_L}{R_T} = \frac{1}{1 + \frac{1}{H_c \frac{k_G a}{k_L a}}} \dots\dots\dots (16)$$

where  $R_L$ ,  $R_T$  = liquid-phase and total mass-transfer resistance (dimensionless); and  $k_G a$ ,  $k_L a$  = liquid-phase and gas-phase mass-transfer coefficients ( $\text{h}^{-1}$ ).

**EXPERIMENTAL METHODS**

A diffused-aeration system (bubble column) was constructed and 14 experiments were performed to validate the  $\Psi_M$  concept. Fig. 4 shows the bubble column, which consisted of a 91.44 cm  $\times$  20.32 cm section of clear plexiglass column equipped with a fine-pore diffuser stone composed of fused crystalline alumina grains with an average pore size 60  $\mu\text{m}$  (Fisher Scientific Co.). The liquid volume was kept at a constant level of 20.1 L and air-flow rates were varied from 0.38 L/min to 2.55 L/min. Air flow was

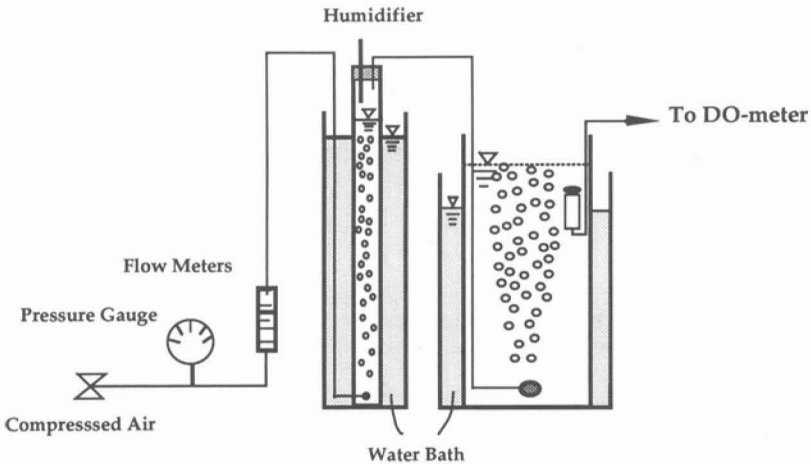


**FIG. 4. Schematic Diagram of Bubble Column and Appurtenances**

**TABLE 2. Summary of Slopes [ $S_p$  (8)] from 14 Experiments**

VOC (1)	Test Number													
	BC9 (2)	BC15 (3)	BC11 (4)	BC3 (5)	BC4 (6)	BC5 (7)	BC6 (8)	BC10 (9)	BC14 (10)	BC7 (11)	BC1 (12)	BC16 (13)	BC12 (14)	BC8 (15)
$[Q_G$ (L/min)]	2.41	2.06	2.10	1.90	1.77	1.77	1.74	1.57	1.41	1.12	1.08	0.92	0.83	0.54
O <sub>2</sub>	15.43	14.5	14.7	14.72	12.62	11.82	13.38	11.09	11.2	9.55	7.34	7.8	7.11	5.35
111TCA	3.208	2.626	3.101	2.593	2.525	2.389	2.344	2.010	1.948	1.591	1.378	1.228	1.211	0.764
PCE	3.490	2.843	3.312	2.577	2.524	2.461	2.402	2.103	1.991	1.498	1.331	1.293	1.207	0.787
CT	5.733	4.955	5.160	4.625	4.122	3.978	4.230	3.618	3.645	2.724	2.360	2.356	2.137	1.449
TCE	1.746	1.449	1.515	1.342	1.290	1.325	1.300	1.114	0.958	0.807	0.712	0.625	0.592	0.391
EBZ	1.752	1.480	1.605	1.372	1.288	1.262	1.247	1.117	1.010	0.799	0.675	0.656	0.606	0.382
12DCE	1.093	0.943	0.990	0.880	0.787	0.779	0.786	0.711	0.654	0.540	0.458	0.424	0.369	0.257
MXY	1.594	1.366	1.404	1.124	1.183	1.157	1.138	0.997	0.958	0.753	0.620	0.606	0.570	0.380
OXY	1.169	0.992	1.026	0.981	0.857	0.840	0.836	0.725	0.685	0.551	0.470	0.467	0.414	0.272
TLN	1.522	1.302	1.331	1.300	1.144	1.118	1.094	0.965	0.849	0.704	0.691	0.585	0.563	0.362
BZ	1.442	1.191	1.248	1.109	1.087	1.097	1.153	0.950	0.837	0.707	0.658	0.556	0.494	0.336
CLF	1.037	0.907	0.923	0.848	0.783	0.801	0.785	0.671	0.633	0.518	0.447	0.418	0.383	0.242
CBZ	0.976	0.840	0.846	0.797	0.731	0.722	0.704	0.636	0.559	0.468	0.429	0.354	0.342	0.231
BBZ	0.661	0.558	0.571	0.540	0.508	0.504	0.500	0.421	0.370	0.326	0.276	0.264	0.236	0.157
13DCB	0.841	0.704	0.728	0.691	0.616	0.616	0.601	0.537	0.496	0.396	0.346	0.328	0.289	0.192
12DCB	0.606	0.525	0.538	0.487	0.445	0.452	0.444	0.388	0.354	0.287	0.234	0.237	0.212	0.139
14DCB	0.744	0.642	0.652	0.603	0.546	0.546	0.533	0.469	0.441	0.348	0.315	0.289	0.258	0.172
BF	0.245	0.190	0.233	0.225	0.217	0.243	0.208	0.154	0.128	0.173	0.155	0.081	0.081	0.048
EDB	0.258	0.185	0.208	0.192	0.186	0.215	0.213	0.179	0.152	0.151	0.128	0.098	0.082	0.060
1122TCA	0.256	0.155	0.202	0.268	0.272	0.208	0.211	0.171	0.100	0.159	0.131	0.056	0.079	0.068
NAPH	0.237	0.168	0.218	0.161	0.231	0.195	0.212	0.171	0.108	0.108	0.123	0.060	0.072	0.055

**TABLE 3. Summary of  $K_L a$  from 14 Experiments**

VOC (1)	Test Number													
	BC9 (2)	BC15 (3)	BC11 (4)	BC3 (5)	BC4 (6)	BC5 (7)	BC6 (8)	BC10 (9)	BC14 (10)	BC7 (11)	BC1 (12)	BC16 (13)	BC12 (14)	BC8 (15)
$[Q_G/V_L (1/h)]$	7.19	6.16	6.27	5.68	5.28	5.28	5.18	4.68	4.21	3.35	3.23	2.75	2.47	1.62
O <sub>2</sub>	16.0	15.1	15.3	15.4	13.2	12.3	14.0	11.6	11.7	10.0	7.6	8.2	7.5	5.7
111TCA	7.17	5.41	9.38	6.08	6.69	5.48	5.37	4.19	4.70	4.12	2.84	2.75	3.55	1.94
PCE	7.97	5.91	9.68	5.22	5.58	5.19	5.02	4.20	4.31	2.96	2.39	2.78	2.80	1.80
CT	10.01	8.73	9.30	8.25	7.05	6.59	7.56	6.14	6.97	4.84	3.82	4.45	4.10	2.90
TCE	6.03	4.21	5.04	3.98	4.62	—	6.91	3.42	2.47	2.62	1.70	1.61	1.90	1.29
EBZ	5.19	4.14	6.80	3.91	3.81	3.45	3.49	3.05	2.80	2.16	1.37	1.79	1.86	1.00
12DCE	2.96	2.62	3.14	2.56	2.00	1.92	2.10	1.92	1.91	1.95	1.03	1.21	0.95	0.84
MXY	4.77	4.09	4.40	2.45	3.70	3.28	3.25	2.58	3.29	2.39	1.28	1.77	2.26	1.94
OXY	2.98	2.46	2.66	3.18	2.17	2.01	2.08	1.64	1.74	1.45	0.95	1.39	1.17	0.77
TLN	4.19	3.57	3.70	—	3.45	3.07	2.97	2.44	2.02	1.88	1.99	1.64	2.79	1.32
BZ	3.55	2.70	3.01	2.56	2.88	3.00	4.84	2.42	2.01	2.05	1.70	1.40	1.21	0.91
CLF	2.67	2.50	2.53	2.46	2.20	2.49	2.43	1.70	1.89	1.81	1.04	1.32	1.39	0.70
CBZ	2.79	2.45	2.36	2.70	2.28	2.12	2.01	1.83	1.47	1.53	1.14	0.86	1.08	0.89
BBZ	1.88	1.51	1.57	1.82	1.86	1.73	1.87	1.11	0.91	1.33	0.64	0.96	0.83	0.62
13DCB	2.57	1.95	2.14	2.81	1.85	1.85	1.76	1.51	1.56	1.27	0.80	1.12	0.89	0.63
12DCB	2.18	2.10	2.34	2.10	1.58	1.88	1.87	1.25	1.24	1.20	0.50	1.14	0.95	0.60
14DCB	2.47	2.24	2.23	2.51	1.79	1.79	1.70	1.33	1.58	1.17	0.82	1.08	0.92	0.71
BF	0.52	0.35	0.61	0.79	—	—	0.82	0.31	0.23	—	—	0.14	0.16	0.09
EDB	0.61	0.33	0.43	0.41	0.42	1.06	—	0.52	0.37	—	0.45	0.23	0.17	0.16
1122TCA	0.57	0.24	0.38	—	—	0.61	0.76	0.40	0.15	—	0.46	0.08	0.15	—
NAPH	0.55	0.30	0.59	0.30	—	0.71	—	0.58	0.18	0.24	—	0.09	0.14	0.14

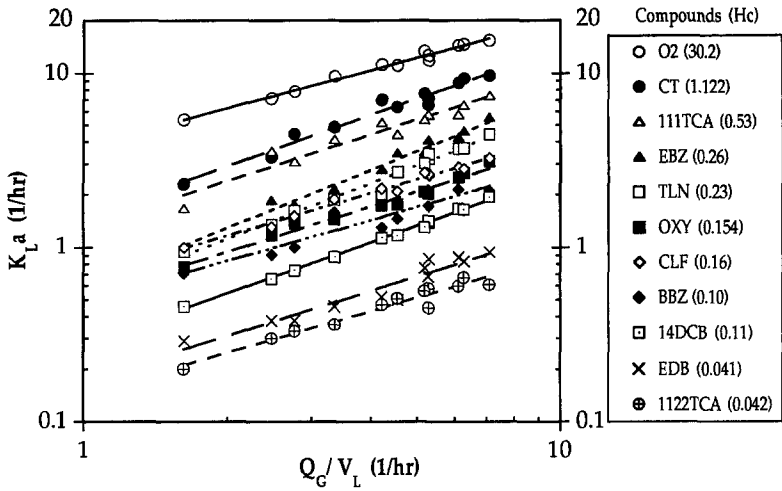


FIG. 5. Mass-Transfer Coefficients as Function of Specific Air-Flow Rate and Henry's Coefficient

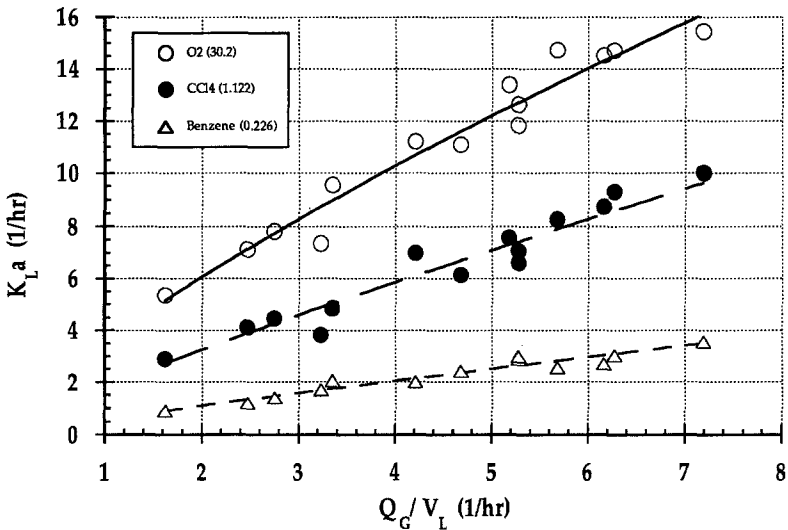
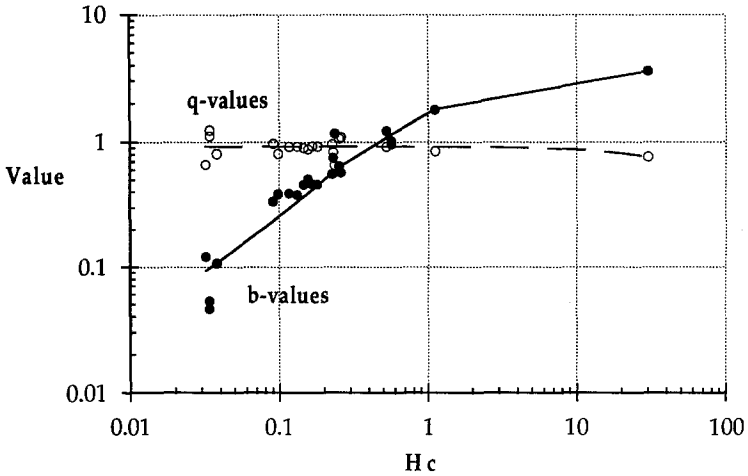
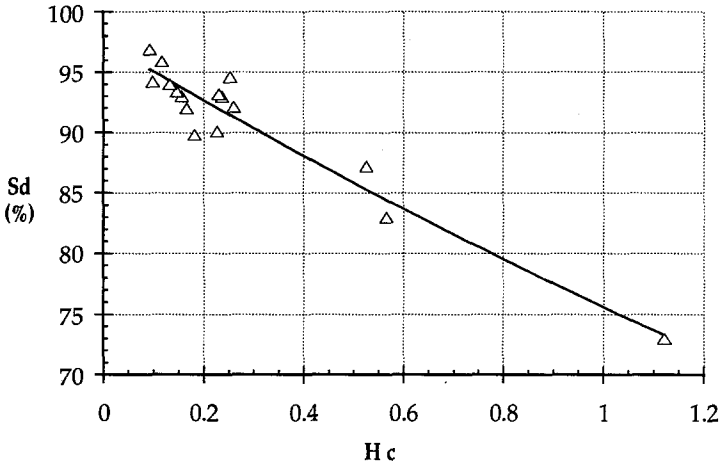


FIG. 6. Mass-Transfer Coefficients versus Specific Air-Flow Rate for Oxygen, Carbon Tetrachloride, and Benzene

measured and controlled by a Cole-Parmer model 3216-45G aluminum flow-meter with an FM 102-05 flow tube (3.175-mm flow tube with glass float). The dissolved oxygen (DO) concentration was measured with a YSI model 58 DO meter, with a probe suspended at 33% of submergence. The ASCE (1984) procedure was used to estimate  $K_L a$ 's. To avoid evaporation, the air flow was passed through a humidifier prior to entering the column. The humidifier was constructed of a 91.44 cm  $\times$  7.62 cm section of clear PVC pipe and filled to the 76.2-cm height with water. The humidifier was equipped



**FIG. 7. Plot of  $b$  and  $q$  from Power Function  $K_{La} = b(Q_G/V_L)^q$  versus Henry's Coefficient**



**FIG. 8. Mean Value (from 14 Experiments) of Degree of Saturation versus Henry's Coefficient for 20 VOCs**

with an air-diffuser stone (same type as those used in the bubble column). The bubble column and the humidifier were immersed in water baths to maintain constant water temperatures of  $20 \pm 0.3^\circ\text{C}$ . A Haake KT 33 circulating water bath was used to maintain the desired temperature in the water baths.

Before the test, the bubble column was washed with tap water and fan dried overnight. Tap water was transferred into the column to the desired volume on the day before the experiment. During filling, a small air-flow rate (approximately 0.13 L/min) was used to provide mixing and to prevent water from entering the diffuser stone and air line. After the water temperature stabilized at  $20^\circ\text{C}$ , the air flow was adjusted to the desired rate.

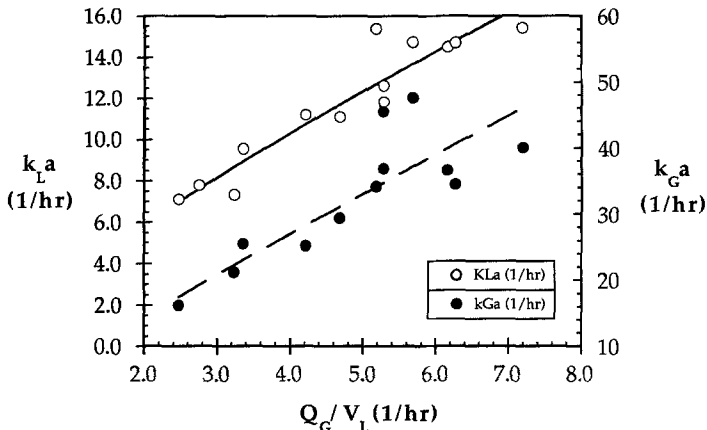


FIG. 9. Dependence of Liquid-Phase and Gas-Phase Mass-Transfer Coefficients on Specific Air-Flow Rate

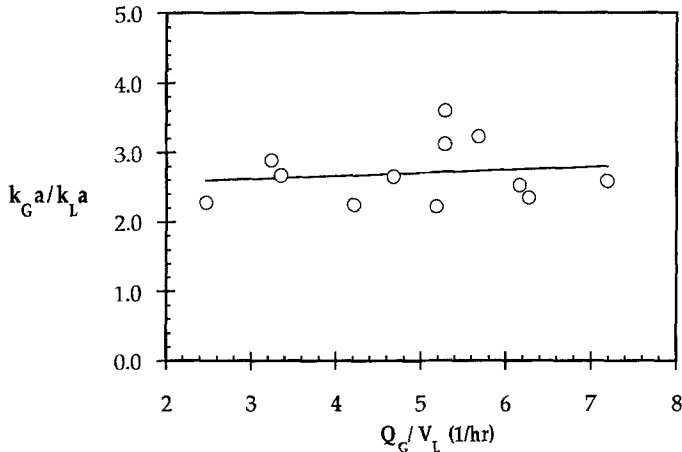


FIG. 10. Ratios of Gas-Phase to Liquid-Phase Mass-Transfer Coefficient versus Specific Air-Flow Rate

Next, sodium sulfite and cobalt chloride were added to deoxygenate the water. After the DO concentration was reduced to almost zero, approximately 5 mL of the VOCs dissolved in methanol was introduced with a pipette, providing approximately 1.0–2.0 mg/L initial concentrations of each VOC. The remaining experimental procedures are the same as those used in the surface-aeration experiments in part 1 (Hsieh et al. 1993). The co-solvent concentration including methanol and 20 VOCs in water (0.26 g/L) used in this study was far below the effective concentration reported by Munz and Roberts (1987). The discussion of this was presented in the surface-aeration experiments (Hsieh et al. 1993).

Table 1 shows the compounds used in this study along with the abbreviations used and some of their properties. The VOC concentrations were measured with a purge-and-trap gas chromatograph (GC). The details of

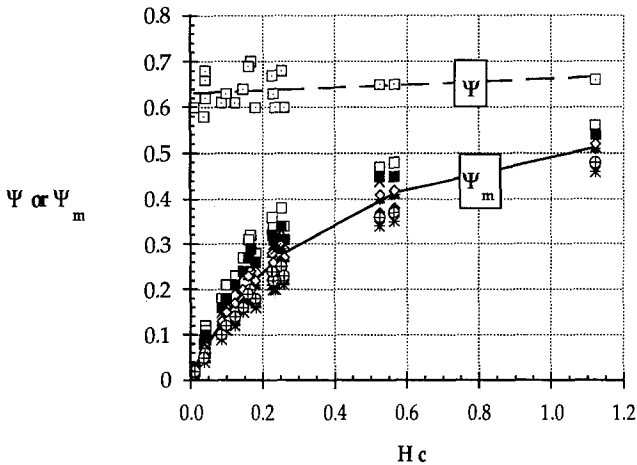


FIG. 11. Comparison of  $\Psi$  and  $\Psi_M$  Values of Various Air-Flow Rates

the analytical procedures and the procedures for calculating the gas-phase and liquid-phase mass-transfer coefficients were described in part 1 (Hsieh et al. 1993).

## RESULTS AND COMMENT

### Mass-Transfer Coefficient and Gas-Phase Saturation

Tables 2 and 3 summarize the slopes [ $Sp$ , see (7) and (8)] of log-linear regressions and  $K_L a$ 's of 20 VOCs and oxygen from the 14 experiments performed at different air-flow rates from 0.54 L/min to 2.41 L/min. It was anticipated that higher  $H_c$ 's would correspond to higher mass-transfer rates. The dependence of  $K_L a$ 's and  $H_c$ 's on the specific air-flow rate ( $Q_G/V_L$ ) is shown in Fig. 5. As Fig. 5 indicates,  $K_L a$  increases with increasing specific air-flow rate ( $Q_G/V_L$ ) as well as increasing  $H_c$ .

The results from Table 3 for  $K_L a$  with different air-flow rates can be fitted with a simple power function of the form,  $K_L a = b(Q_G)^q$ . Fig. 6 is an example plot of  $K_L a$  versus  $Q_G$  for oxygen, carbon tetrachloride, and benzene. The values of coefficient  $b$  and exponent  $q$  for all 20 VOCs and oxygen are plotted in Fig. 7. The exponents  $q$  in the power function are all very close to 1.0 over a wide range of  $H_c$  (0.04–30.2). The nearly constant exponent of 1.0 indicates that the relationship between  $K_L a$  and  $Q_G/V_L$  is linear. For  $H_c < 1.2$ , the approximately linear increase of the coefficient  $b$  with  $H_c$  implies that higher  $H_c$ 's correspond to higher  $K_L a$ 's.

Fig. 8 shows the mean values of  $Sd$  (from 14 experiments) for each compound versus its  $H_c$ . As can be seen in Fig. 8,  $Sd$  increases with decreasing  $H_c$  because for low-volatility compounds, the equilibrium gas-phase concentration is small and thus saturation is achieved rapidly.

### Ratio of Gas- to Liquid-Transfer Coefficients

Fig. 9 shows  $k_G a$  and  $k_L a$  obtained using the nonlinear regression procedure described previously (Hsieh et al. 1993) versus specific air-flow rate, and Fig. 10 shows  $k_G a/k_L a$  versus specific air-flow rate. Fig. 9 shows that both  $k_G a$  and  $k_L a$  are proportional to specific air-flow rate. The gas-phase

TABLE 4. Calculated and Measured Mass-Transfer Coefficients

Compound (1)	Test BC9; Ratio 2.28; <i>n</i> = >0.5			Test BC15; Ratio 3.07; <i>n</i> = >0.5			Test BC3; Ratio 5; <i>n</i> = >0.5			Test BC4; Ratio 3.07; <i>n</i> = >0.5			Test BC5; Ratio 4.11; <i>n</i> = >0.5		
	<i>K<sub>L</sub>a<sup>a</sup></i> (2)	<i>K<sub>L</sub>a<sup>b</sup></i> (3)	ARE <sup>c</sup> (4)	<i>K<sub>L</sub>a<sup>a</sup></i> (5)	<i>K<sub>L</sub>a<sup>b</sup></i> (6)	ARE <sup>c</sup> (7)	<i>K<sub>L</sub>a<sup>a</sup></i> (8)	<i>K<sub>L</sub>a<sup>b</sup></i> (9)	ARE <sup>c</sup> (10)	<i>K<sub>L</sub>a<sup>a</sup></i> (11)	<i>K<sub>L</sub>a<sup>b</sup></i> (12)	ARE <sup>c</sup> (13)	<i>K<sub>L</sub>a<sup>a</sup></i> (14)	<i>K<sub>L</sub>a<sup>b</sup></i> (15)	ARE <sup>c</sup> (16)
O <sub>2</sub>	15.43	19	—	14.5	15.5	—	14.7	12	—	12.62	12.62	—	11.82	10.500	—
111TCA	7.17	6.774	5.5	5.41	6.259	15.7	6.08	5.366	11.7	6.68	5.140	23.1	5.48	4.695	14.3
PCE	7.97	6.958	12.7	5.91	6.395	8.2	5.22	5.456	4.5	5.57	5.250	5.7	5.19	4.774	8.0
CT	10.01	9.034	9.8	8.73	7.944	9.0	8.25	6.522	21.0	7.05	6.501	7.8	6.59	5.706	13.4
TCE	6.03	4.682	22.3	4.21	4.566	8.5	3.98	4.123	3.6	4.61	3.765	18.3	3.90	3.608	7.5
EBZ	5.18	4.238	18.2	4.14	4.124	0.4	3.91	3.715	5.0	3.80	3.400	10.5	3.44	3.251	5.5
12DCE	2.95	3.673	24.5	2.62	3.684	40.6	2.56	3.426	33.8	2.00	3.044	52.2	1.92	2.998	56.2
MXY	4.77	3.978	16.6	4.09	3.897	4.7	2.45	3.536	44.3	3.71	3.215	13.3	3.28	3.094	5.7
OXY	2.98	3.322	11.5	2.46	3.314	34.7	3.18	3.064	3.7	2.16	2.737	26.7	2.01	2.681	33.4
TLN	4.20	4.130	1.7	3.57	4.054	13.5	7.04	3.685	47.7	3.45	3.344	3.1	3.06	3.224	5.4
BZ	3.56	4.347	22.1	2.70	4.271	58.2	2.56	3.887	51.9	2.88	3.524	22.4	3.00	3.402	13.4
CLF	2.67	3.503	31.2	2.50	3.522	40.9	2.46	3.284	33.5	2.21	2.911	31.7	2.49	2.874	15.4
CBZ	2.80	3.023	8.0	2.44	3.056	25.3	2.70	2.867	6.2	2.27	2.527	11.3	2.13	2.509	17.8
13DCB	1.89	2.543	34.6	1.51	2.596	71.9	1.82	2.460	35.2	1.86	2.148	15.5	1.73	2.153	24.4
12DCB	2.56	1.907	25.5	1.95	1.982	1.6	2.81	1.917	31.8	1.85	1.642	11.2	1.85	1.677	9.3
14DCB	2.18	2.287	4.9	2.09	2.348	12.4	2.10	2.242	6.8	1.57	1.945	23.9	1.91	1.962	2.7
BBZ	2.47	2.194	11.2	2.24	2.265	1.1	2.51	2.176	13.3	1.80	1.877	4.4	1.79	1.904	6.4
BF	0.54	1.076	—	0.36	1.148	—	0.88	1.146	—	—	0.954	—	—	1.003	—
EDB	0.61	1.102	—	0.33	1.176	—	0.40	1.175	—	0.42	0.977	—	0.96	1.028	—
112TCA	0.56	1.033	—	0.24	1.101	—	—	1.099	—	—	0.915	—	0.60	0.962	—
NAPH	0.54	0.882	—	0.29	0.943	—	0.29	0.944	—	—	0.783	—	0.66	0.826	—
[M error]	—	—	16.3	—	—	21.7	—	—	22.1	—	—	17.6	—	—	14.9

<sup>a</sup>Measured *K<sub>L</sub>a*.

<sup>b</sup>Calculated *K<sub>L</sub>a*.

<sup>c</sup>Absolute relative error.

TABLE 5. Calculated and Measured Mass-Transfer Coefficients

Compound (1)	Test BC6; $k_G/k_{La}$ 3.14; $n = >0.5$			Test BC10; $k_G/k_{La}$ 2.41; $n = >0.5$			Test BC14; $k_G/k_{La}$ 2.06; $n = >0.5$			Test BC7; $k_G/k_{La}$ 3.9; $n = >0.5$			Test BC12; $k_G/k_{La}$ 2.38; $n = >0.5$		
	$K_{La}^a$ (2)	$K_{La}^b$ (3)	ARE <sup>c</sup> (4)	$K_{La}^a$ (5)	$K_{La}^b$ (6)	ARE <sup>c</sup> (7)	$K_{La}^a$ (8)	$K_{La}^b$ (9)	ARE <sup>c</sup> (10)	$K_{La}^a$ (11)	$K_{La}^b$ (12)	ARE <sup>c</sup> (13)	$K_{La}^a$ (14)	$K_{La}^b$ (15)	ARE <sup>c</sup> (16)
O <sub>2</sub>	13.38	11.5	—	11.09	11.09	—	11.2	12.5	—	9.55	9.55	—	7.11	8	—
11TCA	5.38	4.684	12.9	4.19	4.053	3.3	4.70	4.250	9.6	4.12	4.199	1.9	3.55	2.908	18.1
PCE	5.02	4.784	4.7	4.20	4.159	1.0	4.31	4.373	1.5	2.96	4.273	44.4	2.81	2.984	6.2
CT	7.56	5.924	21.6	6.14	5.354	12.8	6.97	5.770	17.2	4.84	5.141	6.2	4.10	3.849	6.1
TCE	3.91	3.431	12.3	3.42	2.830	17.3	2.47	2.885	16.8	2.63	3.197	21.6	1.90	2.026	6.6
EBZ	3.50	3.098	11.5	3.05	2.560	16.1	2.80	2.613	6.7	2.16	2.882	33.4	1.87	1.833	2.0
12DCE	2.10	2.774	32.1	1.92	2.231	16.2	1.91	2.243	17.4	1.95	2.642	35.5	0.95	1.595	67.9
MXY	3.26	2.929	10.1	2.58	2.406	6.7	3.29	2.447	25.6	2.40	2.739	14.1	2.26	1.722	23.8
OXY	2.08	2.494	19.9	1.64	2.016	22.9	1.74	2.032	16.8	1.45	2.365	63.1	1.17	1.442	23.2
TLN	2.97	3.047	2.6	2.44	2.499	2.4	2.02	2.539	25.7	1.88	2.853	51.8	2.79	1.788	35.9
BZ	4.84	3.211	33.7	2.42	2.631	8.7	2.01	2.671	32.9	2.05	3.010	46.8	1.21	1.882	55.6
CLF	2.43	2.653	9.2	1.70	2.129	25.2	1.89	2.138	13.1	1.81	2.531	39.9	1.39	1.522	9.5
CBZ	2.01	2.303	14.6	1.83	1.839	0.5	1.47	1.841	25.3	1.53	2.207	44.3	1.08	1.314	21.7
13DCB	1.86	1.957	5.2	1.11	1.550	39.6	0.91	1.545	69.7	1.33	1.891	42.1	0.83	1.107	33.4
12DCB	1.75	1.497	14.5	1.51	1.166	22.8	1.56	1.152	26.1	1.27	1.467	15.5	0.89	0.832	6.5
14DCB	1.87	1.772	5.2	1.25	1.395	11.6	1.24	1.386	11.8	1.20	1.721	43.4	0.95	0.996	4.9
BBZ	1.69	1.710	1.2	1.33	1.340	0.7	1.58	1.328	16.0	1.17	1.668	42.6	0.92	0.957	4.0
BF	0.98	0.869	—	0.32	0.661	—	0.24	0.645	—	—	0.872	—	0.17	0.471	—
EDB	—	0.890	—	0.50	0.677	—	0.36	0.661	—	—	0.894	—	0.17	0.483	—
1122TCA	0.73	0.834	—	0.40	0.634	—	0.15	0.619	—	—	0.836	—	0.15	0.452	—
NAPH	—	0.714	—	0.55	0.542	—	0.18	0.528	—	0.24	0.718	—	0.14	0.386	—
[M error]	—	—	13.2	—	—	13.0	—	—	20.8	—	—	34.2	—	—	20.3

<sup>a</sup>Measured  $K_{La}$ .

<sup>b</sup>Calculated  $K_{La}$ .

<sup>c</sup>Absolute relative error.

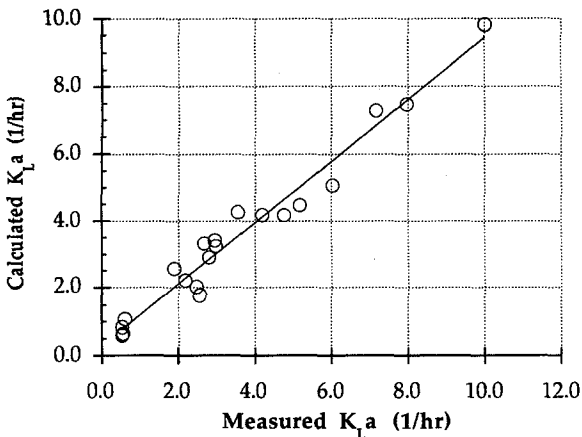


FIG. 12. Comparison between Calculated and Measured Mass-Transfer Coefficients of 20 VOCs (Test Number BC9, Specific Air-Flow Rate = 7.2 L/h)

TABLE 6. Parameters  $a$  and  $b$  for Predicting Transfer Coefficients of VOCs

Test number (1)	$Q_G/V_L$ (2)	$a$ (3)	$b$ (4)	$R$ (5)
BC7	3.55	0.518	1.086	0.965
BC14	4.21	0.348	0.887	0.972
BC12	4.68	0.126	0.954	0.987
BC5	5.28	0.403	0.900	0.980
BC15	6.16	0.558	0.906	0.974

hydrodynamic conditions in the bubble column varied with the specific air-flow rate. The specific air-flow rates used in this study ranged from 2.47/h to 7.19/h, which produced  $k_G a$ 's ranging from 16/h to 48/h (see Fig. 9). From a power-function regression, the  $k_G a$ -values are proportional to  $(Q_G/V_L)^{0.90}$  and the  $k_L a$ -values are proportional to  $(Q_G/V_L)^{0.81}$ . The value of  $k_G a$  increases with increasing air-flow rate because the volume of air increases, which increases the mass-transfer rate. This is unlike a surface-aeration system, in which power input does not increase the volume of air added and the value of  $k_G a$  remains constant. Fig. 10 shows that the  $k_G a/k_L a$  ratios were relatively constant between 2.2 and 3.6 because of the parallel fit of  $k_G a$  and  $k_L a$  to  $(Q_G/V_L)$  shown in Fig. 9. The ratios obtained here for the diffused-aeration system (2.2–3.6) were much smaller than those resulting from surface-aeration experiments (38–110) (Hsieh et al. 1993). This implies that the gas-phase resistance in the bubble column is extremely important and cannot be neglected (as it is when  $\Psi$  is used in place of  $\Psi_M$ ).

#### $\Psi_M$ -Value

Fig. 11 shows a comparison of  $\Psi$ - and  $\Psi_M$ -values for 20 VOCs in 10 experiments. Fig. 11 indicates that  $\Psi_M$ -values decrease with decreasing  $H_c$ , while the value of  $\Psi$  remains almost constant. The results show that  $\Psi$  is only valid when the liquid-phase resistance dominates mass transfer, whereas  $\Psi_M$  can be used for compounds with a wide range of volatilities.

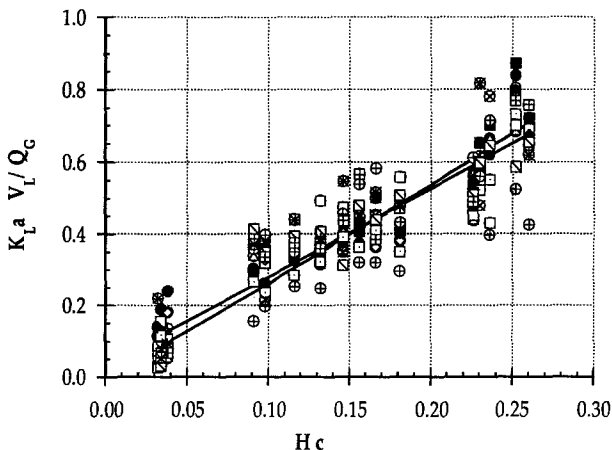


**FIG. 13. Correlation of  $K_L a / Q_G$  and Henry's Coefficient for 14 Experiments with  $H_c < 0.30$**

A comparison of measured and calculated  $K_L a$ 's of 20 VOCs for air-flow rates from 0.83 L/min to 2.41 L/min is shown in Tables 4 and 5. The calculated  $K_L a_{VOC}$ 's were obtained using (14). The values of  $\Psi_M$  in (14) were obtained using (15) and (16). The ratios of  $k_G a$  and  $k_L a$  were obtained using the nonlinear regression procedure described in part 1 (Hsieh et al. 1993). The values of  $K_L a_{O_2}$  were measured simultaneously with the measured  $K_L a_{VOC}$ 's. Fig. 12 is a plot of one of the columns from Tables 4 and 5, which shows good agreement between calculated and measured  $K_L a_{VOC}$ 's for each of the 20 VOCs at a specific air-flow rate of 7.2/h. Table 6 shows regression and correlation coefficients ( $R$ ), between measured and calculated  $K_L a_{VOC}$ 's over the range of specific air-flow rates tested. The proportionality between calculated and measured  $K_L a_{VOC}$ 's ranged from 0.9 to 1.08 (ideally, it should equal 1.0). All of the intercepts are high, with a range from 0.13 to 0.56 (ideally should equal 0.0), due to an overestimation of  $K_L a_{O_2}$  or an underestimation of  $K_L a_{VOC}$  because of the saturation phenomenon of VOCs in the bubbles. The discrepancy between measured and calculated values of  $K_L a_{VOC}$ 's (excluding EDB, bromoform, 1,1,2,2-TCA, and naphthalene) over a series of tests were large (from 13% to 34.2%). The major reason for the high variances is the large value of the intercepts. Other errors may arise from the experimental method used for measuring  $K_L a_{O_2}$  and  $K_L a_{VOC}$ , and error in estimates for liquid diffusivity, which were discussed in part 1 (Hsieh et al. 1993).

### Approximation Method for Field Application

The  $\Psi_M$  concept can be used to estimate the VOC stripping rate when the oxygen-transfer coefficient is known. In cases in which the mass-transfer coefficient is not known, further simplifications can be made in order to develop an approximation method that can be used in field applications.

Earlier in this paper it was noted that the oxygen-transfer coefficient is proportional to specific air-flow rate [ $K_L a \propto (Q_G/V_L)$ ]. For specific applications in which this is true, such as the bubble column described in this paper and similar processes, such as a fine-pore aeration system, we can

assume that  $K_L a [(Q_G/V_L)]$  is approximately constant. In effect it becomes a dimensionless parameter.

The dimensionless parameter can be correlated to  $H_c$ , as follows:

$$\frac{K_L a_{\text{VOC}}}{\left(\frac{Q_G}{V_L}\right)} = b(H_c)^q \dots\dots\dots (17)$$

Eq. (17) is very similar to (10), rewritten as follows to show the similarity:

$$\frac{K_L a_{\text{VOC}}}{\left(\frac{Q_G}{V_L}\right)} = -\ln(1 - Sd)H_c \dots\dots\dots (18)$$

If the value of  $q$  were unity and  $b$  was equal to  $-\ln(1 - Sd)$ , (17) and (18) would be identical. The best-fit estimates of  $b$  and  $q$  for the experiments reported in Table 2 were 2.9 and 1.04, respectively (correlation coefficient,  $R = 0.92$ ), and are shown in Fig. 13. The value of  $q$  is very close to 1.0. The value of  $b$  ranged from 0.7 to 5.0, averaging 2.5, which approximates the best-fit estimate for  $b$  of 2.9. Therefore the empirical and theoretical approaches provide very similar results.

Truong and Blackburn (1984) developed a similar correlation but used the slope [(8)]. Roberts et al. (1982) also showed this correlation for high-volatility compounds.

This research extends the aforementioned concept to low- and medium-volatility compounds. Eq. (18) may be useful when precise results are not required or when insufficient information or funds are available to obtain precise results.

**CONCLUSIONS**

Good correlation between estimated and measured values of  $K_L a$  of 20 VOCs was observed when using the  $\Psi_M$  approach. The results indicate that  $\Psi_M$  is useful for estimating  $K_L a$  for VOCs over a wide range of volatilities or Henry's coefficients.

The  $K_L a$ 's of 20 VOCs were correlated to specific air-flow rates. The results indicate that the relationship between  $K_L a$  and  $Q_G/V_L$  is approximately linear.

The values of  $k_G a/k_L a$  for oxygen were relatively constant, ranging from 2.2 to 3.6 for experiments because of the proportionality relationship between  $k_G a$  and  $k_L a$ . The ratios obtained were much smaller than those observed in surface aeration experiments (38–110). This implies that gas-phase resistance in the diffused-aeration column is extremely important. Gas-phase resistance becomes increasingly more important as  $H_c$  decreases.

A method for approximating VOC stripping using only gas-flow rate per unit volume and Henry's coefficient was presented.

**ACKNOWLEDGMENTS**

This research was supported in part by the NSF-funded Engineering Research Center for Hazardous Substance Control at UCLA and a fellowship from BP-America. We acknowledge Dr. Jack Lee of the UCLA Office of Academic Computing for his help with the SAS model used to analyze the

data, and special thanks to Eddy C. T. Tzeng for his assistance in GC analyses. We thank Dr. Judy A. Libra for her contributions.

## APPENDIX I. REFERENCES

- ASCE Oxygen Transfer Standards Committee. (1984). *A standard for the measurement of oxygen transfer in clean water*. ASCE, New York, N.Y.
- Hsieh, C.-C., Ro, K. S., and Stenstrom, M. K. (1993). "Estimating emission of 20 VOCs. I: Surface Aeration." *J. Envir. Engrg.*, ASCE, 119(6), 1077-1098.
- Mackay, D., Shiu, W. Y., and Sutherland, R. P. (1979). "Determination of air-water Henry's law coefficients for hydrophobic pollutants." *Envir. Sci. Technol.*, 13(3), 333-337.
- Matter-Mueller, C., Gujer, W., and Giger, W. (1981). "Transfer of volatile substances from water to the atmosphere." *Water Res.*, 15(11), 1271-1279.
- Munz, C., and Roberts, P. V. (1984). "The ratio of gas phase to liquid phase mass transfer coefficients in gas-liquid contacting processes." *Gas transfer at water surfaces*, W. Brutsaert and G. H. Jirka, eds., D. Reidel Publishing Co., Hingham, Mass., 35-45.
- Munz, C., and Roberts, P. V. (1987). "Air-water phase equilibria of volatile organic solutes." *J. AWWA*, 79(1), 62-69.
- Roberts, P. V., Munz, C., Dandilker, P., and Matter-Mueller, C. (1982). "Volatilization of organic pollutants in wastewater treatment-model studies." *EPA-600/S2-84-047*, U.S. EPA, Cincinnati, Ohio.
- Roberts, P. V., Munz, C., and Dandilker, P. (1984). "Modeling volatile organic solute removal by surface and bubble aeration." *J. WPCF*, 56(2), 157-163.
- Truong, K. N., and Blackburn, J. W. (1984). "The stripping of organic chemicals in biological treatment processes." *Envir. Prog.*, 3(3), 143-152.

## APPENDIX II. NOTATION

*The following symbols are used in this paper:*

- $a$  = interfacial area;
- $C$  = concentration;
- $D$  = diffusivity;
- $f_{K_r a}$  = transfer parameter;
- $\bar{H}_c$  = dimensionless Henry's coefficient;
- $K$  = overall mass-transfer coefficient;
- $k$  = mass-transfer coefficient;
- $n$  = exponent of liquid diffusivity;
- $p$  = vapor pressure;
- $Q$  = flow rate;
- $q$  = power-function exponent;
- $R$  = film resistance;
- $S$  = solubility;
- $S_d$  = degree of saturation;
- $Sp$  = slope;
- $t$  = time;
- $tr$  = total bubble-travel time;
- $V$  = volume;
- $Z$  = depth;
- $Z_s$  = diffuser depth;
- $\phi Z_s$  = saturation parameter;

$\Psi$  = ratio of mass-transfer coefficients of VOC to oxygen; and  
 $\Psi_M$  = modified  $\Psi$ .

**Subscripts**

$G$  = denotes gas phase;  
 $L$  = denotes liquid phase;  
 $o$  = denotes initial;  
 $O_2$  = denotes oxygen;  
 $T$  = denotes total; and  
VOC = denotes volatile organic compound.

**Superscript**

\* = denotes saturation.